International Conference on Computational Methods in Marine Engineering
MARINE 2011
L.Eça, E. Oñate, J. García, T. Kvamsdal and P. Bergan (Eds)

NUMERICAL SIMULATION OF AN OSCILLATING WATER COLUMN WAVE ENERGY CONVERTER WITH AND WITHOUT DAMPING

MARINE 2011

E. DIDIER[+, *, †], J.M. PAIXÃO CONDE[*, ‡] AND P.R.F. TEIXEIRA[#]

[+] Laboratório Nacional de Engenharia Civil (LNEC)
Av. do Brasil, 101, 1700-066, Lisboa, Portugal
Email: edidier@lnec.pt - web page: http://www.lnec.pt

[*] Faculdade de Ciências e Tecnologia – Universidade Nova de Lisboa (FCT-UNL)
2829-516, Monte de Caparica, Portugal
Email: jpc@fct.unl.pt - Web page: http://www.fct.unl.pt

[†] MARETEC – IST, Universidade Técnica de Lisboa
Av. Rovisco Pais, 1049-001, Lisboa, Portugal
Web page: http://maretec.ist.utl.pt/marine_technology.htm

[‡] IDMEC – IST, Universidade Técnica de Lisboa
Av. Rovisco Pais, 1049-001, Lisboa, Portugal
Web page: http://www.idmec.ist.utl.pt

[#] Universidade Federal de Rio Grande (FURG)
Av. Italia, km 8, Campus Carreiros, 96201-900, Rio Grande, RS, Brazil
Email: pauloteixeira@furg.br - web page: http://www.furg.br

Key words: Wave Energy Converter, Oscillating water column, Numerical simulation.

Summary. This paper presents numerical simulations that predict the action of a regular incident wave on a simplified Oscillating Water Column Ocean Wave Energy Converter (OWC-OWEC) model. This model is a vertical tube of small circular cross-section placed in the longitudinal symmetry plane of the flume. The paper presents a comparison of numerical results, obtained by a Reynolds-Average-Navier-Stokes (RANS) solver, with experimental data obtained in a wave flume. The numerical code uses a finite-volume method to solve the RANS equations and the Volume of Fluid (VOF) approach to capture the water free surface.
The OWC power output is estimated by the pressure drop across the dissipative device (turbine) times the volume flow rate. In the physical model, the turbine's damping effect was simulated by a piece of porous membrane (textile) placed at the top of the vertical tube. To simulate this dissipative effect in the numerical simulations, a pressure drop at the top boundary of the vertical cylinder was imposed. The water free-surface elevation time-series, inside and outside of the cylinder, and the resulting amplification factor obtained by the numerical code are compared with the experimental data for a regular incident wave with 0.015m height and frequency between 0.55 and 1.6Hz. Good concordance is obtained between numerical and experimental results, as it was also found in previous studies for the same configuration without damping.

1 INTRODUCTION

The potential for ocean wave energy utilization is capable of covering a large part of the European consumption of electricity, if extensive use is made of the resource. The use of wave energy along the coastal areas is a particularly attractive option in high-latitude regions. Along the coasts of northern Europe, North America, New Zealand, Chile and Argentina, for instance, are found high densities of annual average wave energy, typically between 40 and 100 kW per m of wave front [1].

Based on various energy extracting methods, a wide variety of systems has been proposed, but only a few full-sized prototypes have been built and deployed in open coastal waters and connected to the electric grid. The Oscillating Water Column (OWC) is considered to be one of the more technically known Ocean Wave Energy Converters (OWEC), due to the large research effort that has been subject in recent years. The OWC-WEC is one of the first to have reached the status of full-sized device deployed in the real sea. Most of the first prototypes were installed in the shoreline. Since the level of the wave energy resource is larger in deep-water locations than close to the shoreline, a natural evolution is the floating OWC in deep water, which, in addition, has the advantage of being less constrained by the geomorphology of the shoreline and less affected by tidal effects.

An OWC-OWEC consists of a partially submerged structure, open below the water free surface. The structure forms a pneumatic chamber at its upper part (above water level). An opening on the submerged part enables the entrance of water into the chamber, and by the effect of incident waves the water free surface inside the chamber is forced to oscillate (oscillating water column), inducing an up-and-down air displacement. The chamber is connected to the atmosphere by an air duct containing a reversible air turbine, e.g. Wells turbine, coupled to an electric generator. The alternating airflow exiting the interior chamber drives the turbine [2]. The closer to the natural frequency of the water column are to the frequencies of the waves, the greater the energy output.

Most of the first prototypes were installed in the shoreline, or in breakwaters, in different parts of the world (Toftestallen, Norway, 1985; Sakata, Japan, 1988; Trivandrum, India, 1990; Pico, Portugal, 1999; Limpet, Scotland, 2000; Port Kembla, Australia, 2005; Mutriku, Spain, 2010).

Although the coastal systems have the advantages of the ease of access and lack of moorings, they have the disadvantage of having lower incident energy, compared with the available offshore, due to dissipative effects of the wave breaking and the seabed friction. The evolution from coastal systems to offshore systems, where the wave energy is higher, is advantageous because the latter are not constrained by the morphology of the coast, or subject to tidal effects.

Some floating OWC systems have already been developed, e.g.: Migthy Whale (Japan), Energetech (Australia), OE buoy (Ireland), Sperboy (England). In the medium to long term, it is expected the installation of floating offshore OWC-OWEC's farms, in areas with depths of 40 to 70 m [3].

It is not common practice to use a single numerical code to simulate all the effects verified in this type of device. This code should accurately simulate the 3D wave propagation and its transformation when subjected to the OWC-OWEC influence; the water inflow and outflow

in the device; the airflow in the pneumatic chamber and the damping caused by the pressure loss at the turbine. A correct simulation of these flows is essential to evaluate the design of the pneumatic chamber and to determine the operating conditions of the turbine [4].

An OWC-OWEC in the form of a vertical tube of small circular cross-section is a geometrically simple point absorber that was been studied analytically and experimentally by many authors.

Evans [5] simulated the water free surface by the motion of a rigid piston without mass for the case of a vertical tube of small diameter in relation to the wavelength. In this theoretical model, the Power Take-off (PTO) is simulated by a linear mass-spring-damper. Falcão and Sarmento [6] and Evans [7] considered an oscillating free surface with uniform pressure distribution. The instantaneous PTO is the product of volumetric flow rate displaced by the free surface and the internal air pressure in the pneumatic chamber. Other authors have used codes based on the Boundary Element Method (e.g. Lee et al. [8]; Brito-Melo [9]; Delauré and Lewis [10]; Josset and Clément [11]; Lopes et al. [12]).

The study of this type of problem is closer to the reality, if a model that considers the complete Reynolds-Average-Navier-Stokes (RANS) equations in the numerical simulations is used. This type of model allows modeling simultaneously the hydrodynamic and aerodynamic flows and the non-linear phonemena between the two phases. Some studies were recently performed using RANS numerical models for investigating OWC device in numerical flume, to reproduce experimental tests and validate numerical models, and also to predict OWC-WEC performance (e.g Wang et al. [13], Alves e Sarmento [14], Hong et al. [15], Horko [16], El Marjani et al. [17], Liu et al. [18, 19], and Davyt et al. [20]).

However, to the best knowledge of the authors of this article, numerical simulations of OWC-OWEC were only performed using potential methods. Only the authors have researched, in previous papers, the numerical simulation of simple offshore OWC-OWEC using RANS models [21, 22, 23]. It was shown that RANS models, like FLUENT [22, 23, 24] and FLUINCO [21, 23], allow to simulate accurately the complex flow outside and inside the OWC device: good concordance was obtained between the two numerical models and experimental results.

This paper presents numerical simulations to predict the action of a regular incident wave on a simplified OWC-OWEC model. This model consists of a vertical tube of small circular cross-section placed in the longitudinal symmetry plane of the flume. In previous studies [21, 22, 23], the top of the vertical cylinder was open to the atmosphere. In the physical model, the turbine's damping effect was obtained by a porous membrane (textile) placed at the top of the vertical tube [12]. So, the OWC power output maybe estimated by the pressure drop across the dissipative device (turbine) times the volume flow rate. To simulate this dissipative effect in the present numerical simulations, a linear law relating the pressure drop to the mass flow rate, is included in the model and imposed as a boundary condition at the top boundary of the vertical cylinder. This simple model allows taking into account the presence of a turbine. The water free-surface elevation time-series, inside and outside of the cylinder, and the resulting amplification factor obtained by the numerical code are compared with the experimental data for a regular incident wave with 0.015m height and frequency between 0.55 and 1.6Hz. As in previous studies, numerical simulations were performed using code FLUENT [24]. This numerical code uses a finite-volume method to solve the RANS equations and captures the

water free surface using the Volume of Fluid (VoF) approach.

2 3D NUMERICAL WAVE FLUME

A fully 3D non-linear numerical model based on Reynolds-Average-Navier-Stokes (RANS) equations and a Volume of Fluid (VOF) technic is used for modeling wave-structure interaction. In the present paper, the numerical model is applied to an OWC-OWEC device model that consists in a vertical tube of small circular cross-section placed in the longitudinal symmetry plane of the flume where damping effect is obtained by a porous membrane (textile) placed at the top of the vertical tube. A linear law relating the pressure drop to the mass flow rate is included in the numerical model and imposed like a boundary condition at the top boundary of the vertical cylinder to take into account the presence of the porous membrane.

2.1 Numerical free surface flow model

The numerical code FLUENT [24] (version 6.3.26), used in the present study, applies the Finite Volume method to solve the set of RANS and VOF equations. The numerical method allows modeling simultaneously the flow of the two phases (water and air) including the non-linear phenomenon which can occurred between the two fluids.

In the FLUENT code, all variables are defined in the center of control volume.

The 3D RANS equations are discretized using an implicit formulation and a second order scheme for time integration.

The diffusive terms of the equations are discretized by the second order central difference scheme. The convective terms of the momentum equation are interpolated at the face of the control volume using the third order scheme MUSCL. The pressure is determined by the PRESTO scheme (PREssure STaggering Option) preferentially used for modeling free surface flow and wave propagation.

The two equations k-ε turbulence model is used in its classical form with standard constants. Convective terms are interpolated at the interfaces by the Second Order Upwind scheme.

The linear system of algebraic equations is solved using the SIMPLEC algorithm that allows velocity and pressure coupling. Under relaxation factors are used only in the equations of k and ε, with the coefficients equal to 0.8.

The free surface capture is done by the VOF method. This method, originally developed by Hirt and Nichols [25], identifies the position of the free surface from a scalar indicator, the volume fraction C, which takes the value 0 in the air and 1 in the water. The position of the free surface is arbitrarily defined by the value 0.5. The transport equation of volume fraction is as follow:

$$\frac{\partial(\mathrm{C})}{\partial \mathrm{t}} + \mathrm{u}.\nabla(\mathrm{C}) = 0 \tag{1}$$

where u is the velocity vector and t the time.

In the present paper, implicit formulation is used with a second order time discretization. The volume fraction on the faces of control volumes is determined by a modified version of the

High Resolution Interface Capturing (HRIC) scheme [26].

2.2 Wave generation

The regular wave is generated by the direct imposition of the free surface elevation and the velocity components, in wave propagation and vertical directions, at the computational domain entry. These conditions are written using a User Defined Function (UDF) [24] based on the velocity profiles and position of the free surface obtained from the linear wave theory.

2.3 Porous membrane model

In the experimental tests, damping effect was obtained by a porous membrane (textile) placed at the top of the vertical tube (OWC model). The porous membrane was used in the physical model because the damping effect is very similar to that obtained by a turbine with linear characteristic, such as the Wells turbine frequently used in OWC devices. A linear law, relating the pressure drop, Δp, to the flow rate at the exit of the vertical tube, Qm, is included in the numerical model using UDFs. Pressure drop is imposed as a boundary condition at the exit boundary of the vertical cylinder to take into account the presence of the porous membrane. Pressure drop is calculated as follow:

$$\Delta p = Ksi \,.Qm\,, \text{ with } \; Qm = \int_S u \; dS \tag{2}$$

where *Ksi* (Pa.s/m^3) is the porous membrane characteristic, *u* the velocity at the exit and *S* the exit area.

2.4 Initial conditions

The initial conditions imposed are the components of the velocity equal to zero in the entire domain (water and air), the hydrostatic pressure that is equal to zero at the free surface, and the free surface flow at still water level.

3 CASE STUDY OF THE OFFSHORE OWC MODEL

3.1 Physical model tests

In this paper, experimental tests described by Lopes et al. (2007) [12] are reproduced to validate the numerical model and demonstrate its application to OWC. The simplified physical model of OWC-OWEC consists of a small vertical hollow cylinder open at the ends and placed vertically (Figure 1). Its axis is coincident with the longitudinal symmetry plane of the flume (0.7m width) and is placed 9.0m from the wave generator. The cylinder has an outer diameter, *D*, and a thickness equal to 0.0550m and 0.0025m, respectively. The water depth, *d*, and wave height, *H*, are equal to 0.40m and 0.03m, respectively.

In the experimental study were considered different submergence lengths, *s*, respectively, 0.100m, 0.180m and 0.245m, different frequencies, *f*, in the range of 0.5~1.6Hz, and tests were made with the top of the cylinder open to the atmosphere and with a pressure loss

(obtained by a porous membrane).

In the frequency range considered for the experimental tests, the ratio d/L (where L is the wavelength) is between 0.11 and 0.66. Only for frequencies above 1.4Hz the incident waves are in deep water condition ($d/L > 0.50$), the remaining are in intermediate depth ($0.50 > d/L > 0.05$) [27].

Although the ratio of outside diameter of the cylinder by the width of the channel is small (~ 7.9%), the experiments do not reflect the effect of a single stand alone device in the open sea, but of an infinite number of devices side by side perpendicularly to the incident waves, because the flume walls act as symmetry planes.

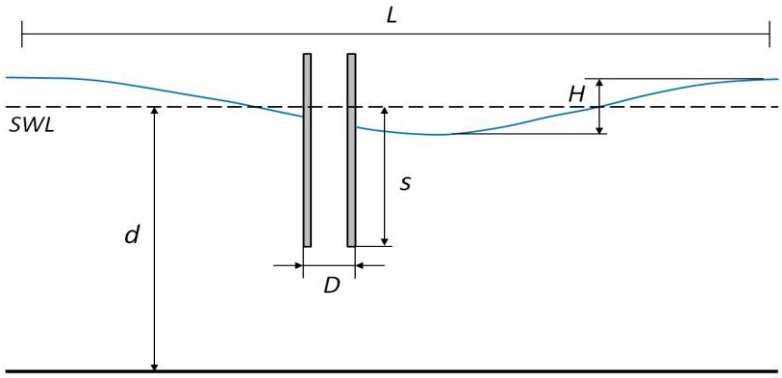

Figure 1: Schematic physical model tests (Lopes et al, 2007) [12] and variables definition.

The flow regime due to wave-structure interaction can be better understood by the calculation of the Keulegan-Carpenter number, $KC = u\,T/D$, where u is the amplitude of the maximum velocity of the flow (in this case the wave velocity at the surface), T is the wave period and D is the outer diameter of the cylinder. The values of KC for the cases studied were between 1.7 and 2.9. In this range of KC, the inertia forces are predominant compared to the drag ($KC < 3$ to a vertical circular cylinder submerged to the bottom).

The ratio D/L is another parameter used to analyze the wave-structure interaction. For the cases studied, this ratio varies from 0.015 to 0.09, with higher values referring to waves of higher frequencies. Note that the higher this ratio, the greater the diffraction effect on the wave transformation (it is considered that to $D/L < 0.2$, the effects of diffraction can be neglected). It is noteworthy that in the present work, the cylinder is partially submerged, which differs from the cases studied by several authors who have established limits for these flow parameters. Furthermore, the cylinder is hollow, which means that an interaction between the mass of fluid inside the cylinder and the external flow exists.

Teixeira et al. [21] and Paixão Conde and Didier [22] found the presence of turbulence in the region near the submerged end of the cylinder, which is the main reason for the use of turbulence models.

Previous studies were carried out by the authors [21, 22, 23] considering only the physical tests without pressure loss and with submergence length equal to 0.18m.

In the present study the authors investigate the same configuration but with additional pressure loss as in the experimental tests.

3.2 Numerical model

In the simulations, taking advantage of the symmetry of the problem in relation to the longitudinal and vertical planes, the computational domain is only half the physical domain. Computational domain extends from one wavelength upstream the vertical cylinder and four wavelengths downstream, with a wave dissipation zone about three wave length to avoid wave-reflection. Figure 2 shows a schematic representation of the numerical flume.

The mesh is composed of approximately 4.9×10^5 control volumes for the higher frequency and 6.8×10^5 control volumes for the lower frequency, being more refined in the vicinity of the cylinder (Figure 3).

The perimeter of cylinder semi-circumference is discretized by 40 segments and mesh refinement is performed in the proximity of the vertical cylinder, in normal and vertical direction.

Mesh discretization must be approximately 60 segments by wavelength, in wave propagation direction x_1, and about 20 segments by wave height, in vertical direction x_2, to accurately propagate waves in the numerical flume.

The time step used was $T/640$ and a maximum of six iterations per time step is imposed. This value is sufficient to reduce all residues to values lower than 10^{-3} [28].

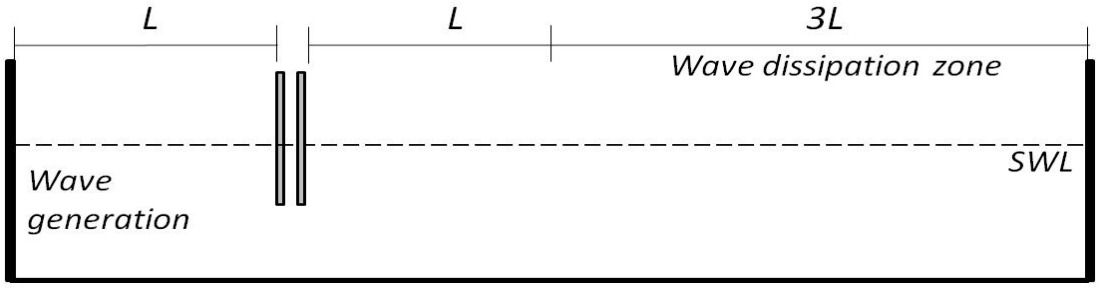

Figure 2: Schematic numerical model of flume.

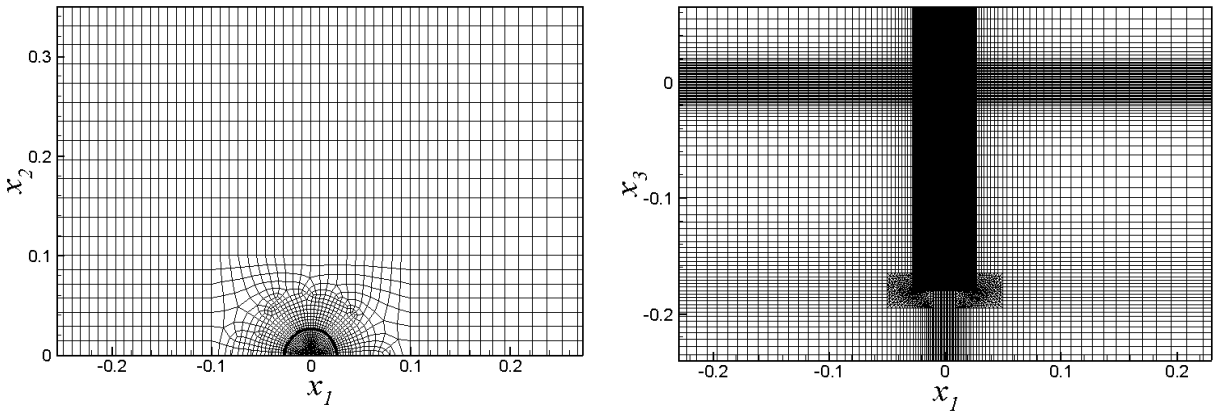

Figure 3: Mesh details in SWL plane and vertical symmetry plane.

4 RESULTS AND DISCUSSION

4.1 Characteristic of the porous membrane

The characteristic of the porous membrane, used in the physical model, was initially unknown. So it is estimated by successive numerical simulations. For each simulation a different value of the porous membrane characteristic *Ksi* was used, and the numerical and experimental free surface elevations inside the OWC, i.e. the wave height inside the OWC, were compared. As soon as the experimental value of wave height is bounded by the upper and the lower values obtained from the numerical simulations, a linear interpolation was used to determine the porous membrane characteristic. Thus, it was found that the porous membrane, used in experiments for modeling the pressure loss, has a characteristic *Ksi* equal to 125Pa.s/m^3.

4.2 Results

For analyzing the free surface, two gauges are placed in the transversal plane coincident with the axis of the cylinder: one is located inside cylinder (in the axis) and the other is outside in an intermediate position between the flume wall and the cylinder wall.

It was found that is necessary approximately a time of about 10 wave-periods to verify that the free surface, measured at the two gauges, will stabilize. After stabilization, it is observed that the free surface elevation inside and outside the cylinder is periodical. Same results are found in [23].

Figures 4a-4f present the time-series of the free surface elevation inside and outside of the cylinder, obtained at two gauges, before resonant frequency (Figures 4a-4c), at resonant frequency (4d) and after resonant frequency (4e-4f). For lower frequencies, 0.5 and 0.6Hz, a second frequency appears inside the vertical cylinder. This effect is responsible for the changing of the amplification factor and phase angle behavior (Figure 5). Similar effect for the frequency 0.6Hz was found by the authors for a device without damping [21, 23] and also observed by Lopes et al. [12]. For remaining frequencies, 0.9 to 1.5Hz, free surface behavior is sinusoidal. At resonant frequency, a large amplification of free surface elevation is found. For higher frequencies, free surface elevation inside the cylinder decreases as the frequency increases.

From the time-series of free surface elevation, it is possible to estimate the amplification factor, Q, ratio between the maximum elevation measured inside and outside of the cylinder, and the phase angle, θ, angular difference between the waves measured outside and inside of the cylinder.

Figure 5 shows the amplification factor and the phase angle for frequencies from 0.5 Hz to 1.6 Hz and the comparison between numerical and experimental results. Figure 5a presents numerical and experimental values of amplification factor for a damping configuration and no-damping [21, 23]. The agreement between numerical and experimental results for damping configuration is very good. Comparing present results with configuration without damping, it can be seen that damping effect does not change the resonant frequency, as it was found in experimental tests.

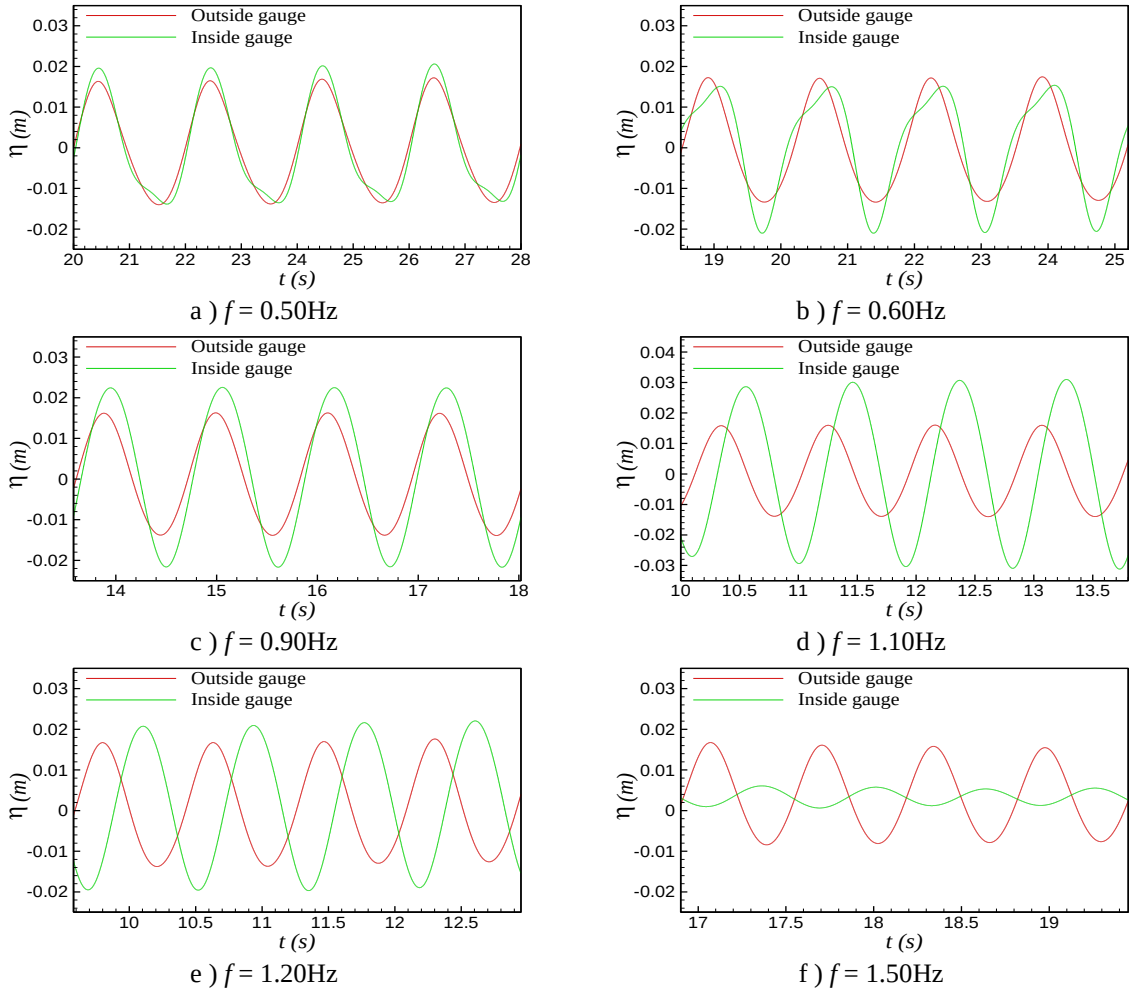

Figure 4: Time series of free-surface elevation outside and inside the OWC cylinder.

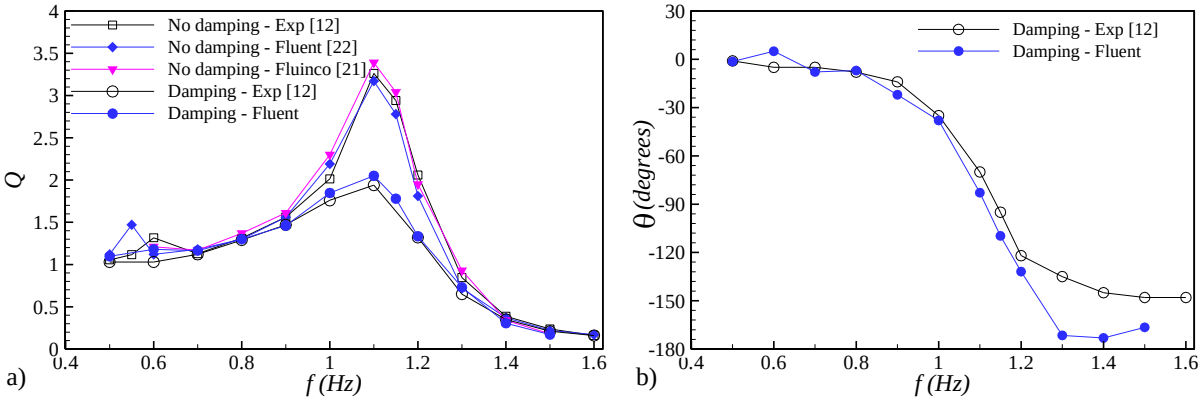

Figure 5: Amplification factor Q (a) and phase angle θ (b) versus the wave frequency.

For a cylinder of small diameter in comparison with its submergence length (s), 0.18 m for studied case, resonance occurs at a frequency $f = (g/s)^{1/2}$, where g is the gravitational

acceleration, resulting f = 7.382rad/s = 1.17Hz.

It can be observed in Figure 5 that the resonant frequency found in both experimental tests and in numerical simulations, for damping and not-damping device, was around 1.1Hz, close to the theoretical value.

Figure 5b presents numerical and experimental values of phase angle for damping device. It can be seen that there is a good concordance between numerical and experimental results on the range 0.7~1.2Hz. However, in the phase transition region, around the resonance frequency (0.9~1.2Hz), numerical code tends to overestimate the phase shift. There is a small difference between the behavior observed for the FLUENT results on range 0.5~0.6Hz and experimental results. In the frequency range 1.2~1.5Hz, numerical results of the phase shift greatly overestimate the experimental data. However, for these higher frequencies, it was showed that amplification factor is well estimated.

5 CONCLUSIONS

This paper presented the results of numerical simulation of an OWC-OWEC using the FLUENT code. The aim of the study was to validate the RANS code for this type of offshore structure, modeling the hydrodynamic and aerodynamic flows simultaneously, in order to apply systematically the numerical model to wave energy converters design.

The simulated case corresponds to a simplified model of an OWC-OWEC tested experimentally in a channel with 0.4m deep and 0.70m wide. The model is a hollow cylinder with outer diameter of 0.055m and thickness of 0.0025m. It was placed in the plane of symmetry of the channel and its submerged part was 0.18m from the still water level. Monochromatic incident waves with 0.030m height and frequencies in the range 0.5~1.6Hz were simulated. In the experimental tests, a damping effect was simulated by a porous membrane (textile) placed at the top of the hollow cylinder. Porous membrane is used in the physical model because the damping effect is very similar to that obtain by a turbine with linear characteristic (such as Wells turbine).

Numerically, a linear law, relating the pressure drop to the flow rate at the exit of the hollow cylinder, is used for taking into account the presence of the porous membrane and simulating the resulting pressure drop. The characteristic of the porous membrane was found by comparing numerical and experimental free surface elevation. The porous membrane has a characteristic *Ksi* equal to 125Pa.s/m^3.

The numerical simulations were performed varying the incident wave frequency in the range 0.5~1.6Hz, which enabled an analysis of the amplification factor and phase angle between the free surface elevation inside and outside the cylinder. The numerical results showed a behavior very similar to the experiments. Resonant frequency is found around 1.1Hz, in very good accordance with experimental and theoretical.

The analysis made in this study show the phenomena that occur in the interactions among an OWC-OWEC (vertical cylinder) and monochromatic waves, considering the fully non-linear RANS equations, where the viscosity and turbulence effects are modeled, which allows simulating simultaneously hydrodynamic and aerodynamic flows and non-linear effects that maybe occurred in the device.

The present numerical model can be easily applied to a real practical case of OWC, taking into account the effect of a turbine on pressure variations, when the characteristic of the turbine is known.

ACKNOWLEDGEMENTS

Eric Didier and José M. Paixão Conde acknowledge the funding of research centers MARETEC and IDMEC. The authors also gratefully acknowledge M.F.P. Lopes for supplying his experimental data.

REFERENCES

[1] M.T. Pontes and A.F.O. Falcão, "Oceans Energies: Resourses and Utilization", *18th World Energy Conference*, Buenos Aires (2001).

[2] J. Falnes, *Ocean waves and oscillating systems. Linear interactions including wave-energy extraction*, Cambridge University Press, Cambridge, UK (2002).

[3] A. Clément, P. Mccullen, A.F.O. Falcão, A. Fiorentino, F. Gardner, K. Hammarlund, G. Lemonis, T. Lewis, K. Nielsen, S. Petroncini, M.T. Pontes, P. Schild, B-O Sjöström, H.C. Sorensen and T. Thorpe, "Wave Energy in Europe: Current Statues and Perspectives", *Renewable and Sustainable Energy Reviews*, **6**, 405-431 (2002).

[4] J.M. Paixão Conde and L.M.C. Gato "Numerical study of the air-flow in an oscillating water column wave energy converter", *Renewable Energy*, **33 (12)**, 2637-2644 (2008).

[5] D.V. Evans, "The oscillating water column wave-energy device", *Journal of the Institute of Mathematics and Applications*, **22**, 423-433 (1978).

[6] A.F.O. Falcão and A.J.N.A. Sarmento, "Wave generation by a periodic surface pressure and its application in wave-energy extraction", *15th Int. Cong. Theor. Appl. Mech.*, Toronto (1980).

[7] D.V. Evans, "Wave-power absorption by systems of oscillating surface pressure distributions", *Journal of Fluid Mechanics*, **114**, 481-499 (1982).

[8] C. H. Lee, J.N. Newman and F.G. Nielsen, "Wave interactions with an oscillating water column", *6th Int. Offshore and Polar Eng. Conf., ISOPE*, Los Angeles, **1**, 82-90 (1996).

[9] A. Brito-Melo, *Modeling and pre-dimensioning of oscillating water column power plants: application to the Pico (Azores) wave power plant*, in Portuguese, PhD Thesis, Instituto Superior Técnico (Lisbon) / École Centrale de Nantes (2000).

[10] Y.M.C. Delaure and A. Lewis, "3D hydrodynamic modeling of fixed oscillating water column wave power plant by a boundary element methods", *Ocean Engineering*, **30**, 309-330 (2003).

[11] C. Josset and A.H. Clément, "A time-domain numerical simulator for oscillating water column wave power plants", *Renewable Energy*, **32**, 1379-1402 (2006).

[12] M.F.P. Lopes, P. Ricci, L.M.C. Gato and A.F.O. Falcão, "Experimental and numerical analysis of the oscillating water column inside a surface-piercing vertical cylinder in regular waves", *7Th European Wave and Tidal Energy Conference*, Porto, Portugal (2007).

[13] D. Wang, M. Katory and Y. Li, "Analytical and experimental investigation on the hydrodynamic performance of onshore wave-power devices", *Ocean Engineering*, **29**, 871-885 (2002).
[14] M. Alves and A.J.N.A. Sarmento, "Non-Linear and Viscous Diffraction Response of OWC Wave Power Plants", *6th EWTEC – European Wave and Tidal Energy Conference*, Glasgow, UK (2005).
[15] K. Hong, S. Shin, D. Hong, H. Choi and S. Hong, "Effects of Shape Parameters of OWC Chamber in Wave Energy Absorption", *ISOPE – International Society of Offshore and Polar Engineering*, Lisbon, Portugal (2007).
[16] M. Horko, *CFD Optimization of an Oscillating Water Column Wave Energy Converter*, Master of Engineering Science Thesis, University of Western Australia, Austrália (2007).
[17] A. El Marjani, F. Castro, M. Bahaji and B. Filali, "3D Unsteady Flow Simulation in na OWC Wave Converter Plant", *ICREPQ'06*, Palma de Mallorca, Spain (2006).
[18] Z. Liu, H. Shi H. and B. Hyun, "Practical design and investigation of the breakwater OWC facility in China", *8th EWTEC – European Wave and Tidal Energy Conference*, Uppsala, Sweden (2009).
[19] Z. Liu, B. Hyun, K. Hong and Y. Lee, "Investigation on Integrated System of Chamber and Turbine for OWC Wave Energy Convertor", *ISOPE – International Society of Offshore and Polar Engineering*, Osaka, Japão (2009).
[20] D. Davyt, P. Teixeira, R. Ramalhais and E. Didier, "Numerical analysis of regular waves over an onshore Oscillating Water Column", *ENCIT 2010 – 13th Brazilian Congress of Thermal Sciences and Engineering*, Uberlandia – MG, Brasil (2010).
[21] P. Teixeira, E. Didier and J.M. Paixão Conde, "Análise Numérica de um Equipamento de Energia das Ondas Tipo OWC", *6as Jornadas Portuguesas de Engenharia Costeira e Portuária*, Funchal-Madeira, Portugal (2009).
[22] J.M. Paixão Conde and E. Didier, "Simulação numérica de um dispositivo de aproveitamento da energia das ondas do tipo coluna de água oscilante", *CIBIM9 – 9º Congresso Ibero-Americano em Engenharia Mecânica*, Las Palmas de Gran Canarias, Spain, **5**, 88-95 (2009).
[23] J.M. Paixão Conde, P.R.F. Teixeira and E. Didier, "Simulação numérica de um dispositivo de aproveitamento da energia das ondas do tipo coluna de água oscilante: comparação de dois códigos numéricos", *IV SEMENGO*, Rio Grande - RG, Brazil (2010).
[24] Fluent 6.3, *User's Guide*, Fluent Inc., USA (2006).
[25] C.W. Hirt and B.D. Nichols, "Volume of fluid VoF method for the dynamics of free boundaries", *J. Comp. Phys.*, **39**, 201-225 (1981).
[26] M. Peric and J.H. Ferziger, *Computational Methods for Fluid Dynamics*, Springer, Second edition (1997).
[27] B. LeMéhauté, *An Introduction to Hydrodynamics and Water Waves*, Springer-Verlag, (1976).
[28] T. Barreiro, E. Didier, L. Gil and M. Alves, "Numerical Simulation of the Nonlinear Flow Generated by the Interaction Between Waves and Punctual Wave Energy Converters", in Portuguese, *III National Conference in Fluid Mechanics, Thermodynamics and Energy*, Bragança, Portugal (2009).